DOI 10.5012/bkcs.2011.32.2.515

Molecular Dynamics of Carbon Nanotubes Deposited on a Silicon Surface *via* Collision: Temperature Dependence

Leton C. Saha, Shabeer A. Mian, Hyojeong Kim, Joyanta K. Saha, Mohammad A. Matin, and Joonkyung Jang*

Department of Nanomaterials Engineering, Pusan National University, Miryang 627-706, Korea
**E-mail: jkjang@pusan.ac.kr*
Received October 28, 2010, Accepted December 1, 2010

We investigated how temperature influences the structural and energetic dynamics of carbon nanotubes (CNTs) undergoing a high-speed impact with a Si (110) surface. By performing molecular dynamics simulations in the temperature range of 100 - 300 K, we found that a low temperature CNT ends up with a higher vibrational energy after collision than a high temperature CNT. The vibrational temperature of CNT increases by increasing the surface temperature. Overall, the structural and energy relaxation of low temperature CNTs are faster than those of high temperature CNTs.

Key Words: Carbon nanotube, Collision, Molecular dynamics, Surface deposition, Relaxation

Introduction

Reinforcement with carbon nanotubes (CNTs) has been widely used in synthesizing composite materials.[1-7] Such composite materials are often deposited on surfaces by means of spraying[8,9] at high velocity (more than several hundred km/s). Cold spraying[10,11] is one of the techniques that is used to prepare CNT based composite materials.[12,13] Before spraying, the CNT composites are heat-treated at high temperature (3000 - 46000 K[8] or 400 - 900 K[12,13]). CNTs suffer from deformation caused by a high velocity impact with surface and heat treatment. It would be interesting to study the dynamics and molecular details for the deformation and energy excitation of CNT in such process. There have been several simulation studies on how temperature affects the structure[14,15] or conductivity[16,17] of a single isolated CNT. We are also aware of simulation studies on the structural stability of CNT colliding with a surface,[18,19,20] but the effect of temperature was not taken into account. Herein, we study how temperature affects the CNT deposition under a high velocity impact with a silicon surface. By varying temperatures of both the CNT and the surface, we dynamically investigate the deformation and energy excitation of the CNT. Our molecular dynamics (MD) simulation shows that the vibrational temperature of CNT after collision increases with raising the surface temperature. A CNT initially equilibrated at low temperature turns out more efficient in relaxing its deformed structure and excited vibrational energy. Interestingly, a low temperature CNT ends up with a higher vibrational temperature after collision than a CNT with a high initial temperature. We ascribe this heat transfer from the surface at high temperature to the CNT at low temperature.

Simulation Details

A (6,6) single-walled CNT impacting on the Si (110) surface is shown in Figure 1a. The CNT, made from 384 C atoms, was 3.8 nm long and 0.81 nm in diameter. The CNT was shown to be delivered onto the surface with a projectile speed, v_p, where the arrow in Figure 1a denotes its direction. v_p was chosen to be 5 km/s which is more than three times higher than that in typical cold spray processes.[12,13] In Figure 1a, the temperature of CNT, T_{CNT}, and the surface temperature, T_{Si}, are 100 and 300 K, respectively. The Si (110) surface consisted of a slab of Si crystal with a thickness of 3.43 nm. The atoms in the bottom layer of the slab were fixed throughout the entire simulation. The surface has lateral dimensions of 15.61 nm × 8.97 nm. The periodic boundary conditions[21] were imposed to emulate a laterally infinite surface. The length of simulation box along the Z direction was taken to be 50 nm, in order to avoid the periodicity in the Z-direction. The total number of Si atoms was 24360 for the surface. The CNT and surface were equilibrated separately (to give desired T_{CNT} and T_{Si}) by running constant temperature (NVT) MD[21] simulations. T_{CNT} values of 100 and 300 K and T_{Si} values of 100, 150, 200, 250 and 300 K were respectively

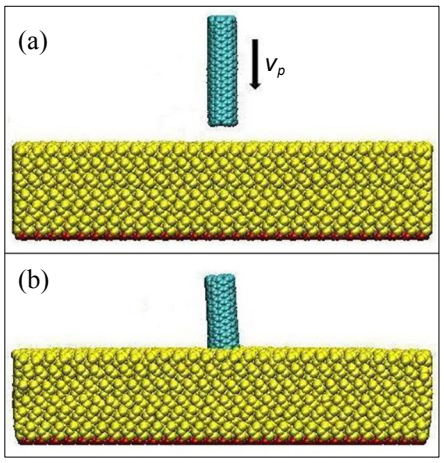

Figure 1. (a) Snapshot of CNT impacting onto a Si (110) surface with a projectile speed of v_p along its axis. The arrow denotes the moving direction of CNT. In this case, T_{CNT} =100 K, T_{Si} = 300 K, and v_p = 5 km/s. (b) Snapshot of CNT penetrated into the surface after collision (at 22 ps after impact).

considered. After being equilibrated to a desired temperature T_{CNT}, a projectile velocity v_p was added to CNT for its collision with the surface. The collision was simulated using a constant energy (NVE) MD method.[21] Figure 1b shows a CNT deposited on the surface after collision (at 22 ps).

We used the Tersoff potential[22] to model the interaction between the CNT and surface. The interatomic potential between atoms *i* and *j*, V_{ij}, is given by

$$V_{ij} = f_C(r_{ij})[V_R(r_{ij}) + b_{ij}V_A(r_{ij})], \quad (1)$$

where r_{ij} represents the interatomic distance. The repulsive and attractive energies, $V_R(r_{ij})$ and $V_A(r_{ij})$, respectively, are represented as,

$$V_R(r_{ij}) = A_{ij}\exp(-\lambda r_{ij}), \quad (2)$$

$$V_A(r_{ij}) = -B_{ij}\exp(-\mu r_{ij}). \quad (3)$$

In equation (1), the cutoff function $f_C(r_{ij})$ limits the interaction as

$$f_C = \begin{cases} 1 & (r_{ij} < R_{ij}) \\ \frac{1}{2} + \frac{1}{2}\cos\left[\frac{\pi(r_{ij} - R_{ij})}{S_{ij} - R_{ij}}\right] & (R_{ij} < r_{ij} < S_{ij}) \\ 0 & (r_{ij} > S_{ij}) \end{cases}. \quad (4)$$

b_{ij} is the bond order of interaction and is given by

$$b_{ij} = \chi_{ij}(1 + \beta_i^{n_i}\xi_{ij}^{n_i})^{-1/2n_i}, \quad (5)$$

with

$$\xi_{ij} = \sum_{k\neq i,j} f_C(r_{ik})\omega_{ik}g(\theta_{ijk}). \quad (6)$$

$g(\theta_{ijk})$ is given by

$$g(\theta_{ijk}) = 1 + \frac{c_i^2}{d_i^i} - \frac{c_i^2}{d_i^2 + (h_i - \cos\theta_{ijk})^2}. \quad (7)$$

All the symbols not explained above are parameters which can be calculated by using the following combination rules:

$$\lambda_{ij} = (\lambda_i + \lambda_j)/2\ , \mu_{ij} = (\mu_i + \mu_j)/2. \quad (8)$$

$$A_{ij} = (A_i A_j)^{1/2}\ , B_{ij} = (B_i B_j)^{1/2}. \quad (9)$$

$$R_{ij} = (R_i R_j)^{1/2}\ , S_{ij} = (S_i S_j)^{1/2}. \quad (10)$$

The parameters, λ_i, μ_i, A_i, B_i, R_i, and S_i, for Si and C are listed in Reference 22.

The MD trajectory was propagated using the velocity Verlet algorithm[21] with a time step of 0.2 or 0.4 fs. The time of impact was defined as the time at which the CNT approaches within 0.178 nm of the surface (0.178 nm is the C-Si distance in a silicon carbide nanotube[23]). The MD simulation typically ran for 22 ps after impact. The above MD methods were implemented using the DL POLY package.[24]

The energy of CNT was analyzed as follows. At each time of simulation, the position and velocity of the center of mass were calculated. The internal position and velocity of the *i* th C atom, $\vec{r}_i$ and $\vec{v}_i$, were obtained by subtracting these values from the position and velocity of each C atom, respectively. The internal kinetic energy K_{int} is given by the sum over each atom as

$$K_{\text{int}} = (m/2)\sum_i \vec{v}_i^{\,2}. \quad (11)$$

The angular momentum $\vec{L}$ and the moment of the inertia tensor *I* were also calculated from $\vec{r}_i$ s and $\vec{v}_i$ s. The rotational kinetic energy K_{rot} and vibrational kinetic energy K_{vib} were calculated as

$$K_{rot} = (1/2)\left(I^{-1}\vec{L}\right)\cdot\vec{L}, \quad (12)$$

$$K_{vib} = K_{\text{int}} - K_{rot}. \quad (13)$$

The vibrational temperature T_{vib} is given by

$$T_{vib} = (2K_{vib})/[(3\times 384 - 6)k_B], \quad (14)$$

where k_B is the Boltzmann constant.

We quantified the deformation of the CNT by calculating the root-mean-squared displacement (RMSD). To do so, the displacement of each C atom from its initial value was calculated. The average of the displacement squared was taken by summing over all the C atoms. We used the numerical method Kabsch[25] implemented in the Visual Molecular Dynamics package.[26]

Results and Discussion

We inspect the snapshots for the deposition of CNT on Si (110) surface which were equilibrated at temperatures of T_{CNT} and T_{Si}, respectively, before collision. Figure 1a shows the CNT impacting on the Si surface at a projectile speed of v_p = 5 km/s. In this case, T_{CNT} and T_{Si} are 100 and 300 K, respectively. Figure 1b shows the CNT penetrated into the Si surface and vertically aligned. Figures 2a-d shows the deformation of CNT for different combinations of T_{CNT} and T_{Si}. In all cases, the CNT penetrated into the Si surface and were vertically aligned on the surface. The deformation was localized around the bottom of the CNT. In the case of T_{CNT} = 100 K and T_{Si} = 100 K, the bottom of CNT is slightly squeezed without much deformation (Figure 2a). As T_{Si} increases to 300 K, the bottom atoms of CNT are significantly displaced from their original positions before collision (Figure 2c). On the other hand, increasing the temperature of CNT from 100 to 300 K does not much affect the deformation: the structure of CNT for T_{CNT} = 300 K and T_{Si} = 100 K (Figure 2b) is similar to Figure 2a (T_{CNT} = 100 K and

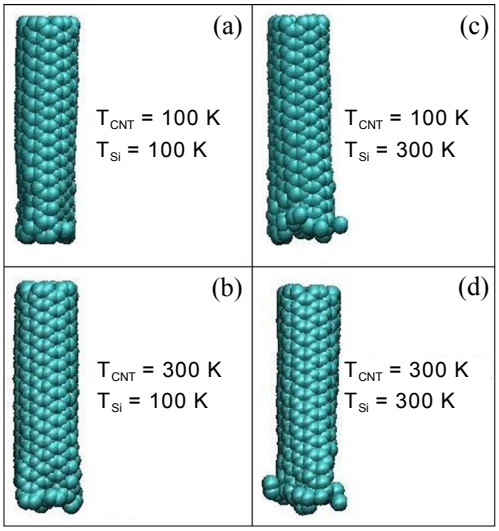

Figure 2. Snapshots of CNTs deformed after collision with Si (110) surface. Shown are four different combinations of the CNT (T_{CNT}) and surface (T_{Si}) temperatures. (a) T_{CNT} = 100 K and T_{Si} = 100 K (b) T_{CNT} = 300 K and T_{Si} = 100 K (c) T_{CNT} = 100 K and T_{Si} = 300 K (d) T_{CNT} = 300 K and T_{Si} = 300 K.

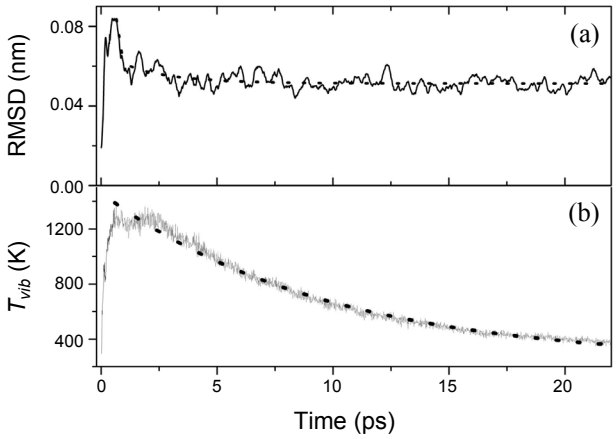

Figure 3. (a) Dynamic deformation of the CNT colliding with the Si (110) surface. For T_{CNT} = 300 K and T_{Si} = 150 K, the RMSD was plotted as a function of time elapsed after impact. The RMSD after its maximum is fitted to an exponential function of time (dotted line). (b) Vibrational temperature, T_{vib}, *vs*. time. T_{vib} after its maximum is fitted to an exponential function of time (dotted line).

T_{Si} = 100 K). The largest deformation of CNT occurs when both the CNT and surface temperatures are high (T_{CNT} = 300 K and T_{Si} = 300 K, Figure 2d). We did not observe any detachment of the atoms from CNT.

In Figure 3, we plot the RMSD and T_{vib} *vs*. time for the case of T_{CNT} = 300 K and T_{Si} = 150 K. After impact (time zero in the figure), both the RMSD and T_{vib} rapidly increase and reach maxima (about 0.085 nm and 1381 K, respectively). These initial increases in RMSD and T_{vib} represent the deformation of CNT and its excitation in vibrational energy, respectively.[20] The maxima in RMSD and T_{vib} are followed by relaxation, in which the RMSD or T_{vib} decreases and levels off to a finite value. This relaxation was modeled by fitting the RMSD and T_{vib} curves to

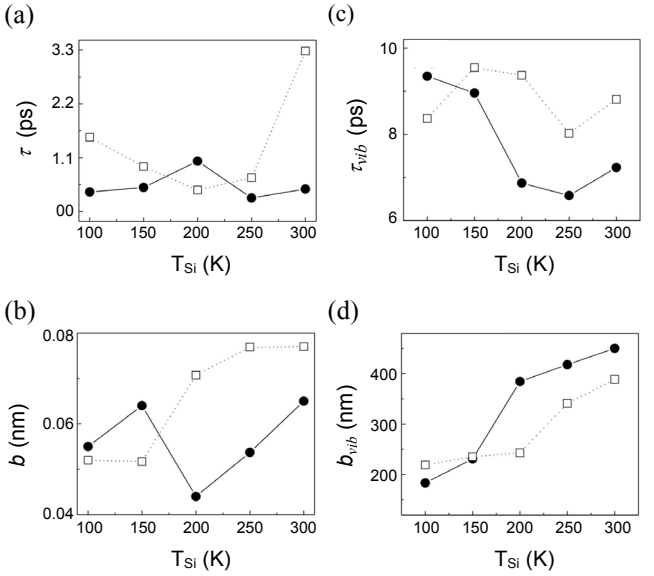

Figure 4. Surface temperature dependence of the deformation and vibrational temperature. In all of the panels, the open squares and filled circles refer to the data obtained for T_{CNT} = 300 K and T_{CNT} =100 K, respectively. Lines are for visual guide. The surface temperature T_{Si} is varied as 100 K, 150 K, 200 K, 250 K and 300 K. (a) The structural relaxation time τ *vs*. T_{Si} (b) The asymptotic RMSD *b vs*. T_{Si}. (c) The vibrational energy relaxation time τ_{vib} *vs*. T_{Si} (d) The long time vibrational temperature b_{vib} *vs*. T_{Si}.

$a \exp(-t/\tau) + b$ and $a_{vib} \exp(-t/\tau_{vib}) + b_{vib}$, respectively (shown as dotted lines in Figures 3a and b). The fitting parameters τ and τ_{vib}, respectively, are called the structural and energy relaxation times of CNT. b_{vib} (529 K in this case) and b (0.14 nm in this case) are the long-time T_{vib} and RMSD which represents the permanent rise in the vibrational temperature and the permanent deformation, respectively.

We calculated the time dependent RMSD and T_{vib} for various combinations of T_{CNT} (100 and 300 K) and T_{Si} (100, 200, 250, and 300 K). The RMSD and T_{vib} curves for each combination were fitted to exponential functions as in Figure 3. Such fittings gave us the relaxation times, τ and τ_{vib}, and the long time values, b and b_{vib} which are shown in Figure 4.

Let us examine the temperature dependence of the deformation dynamics of CNT. Figure 4a plots the structural relaxation time τ *vs*. T_{Si} for T_{CNT}s of 100 K (filled circles) and 300 K (open squares). τ ranges from 0.4 to 3.3 ps for T_{CNT} = 300 K and from 0.4 to 1.0 ps for T_{CNT} =100 K. Overall, τ s for T_{CNT} = 300 K are larger than those for T_{CNT} = 100 K, indicating the structural relaxation of the low temperature CNT is faster. The dependence of τ on T_{Si} is opposite for the high and low temperature CNTs: τ of the high temperature CNT is minimal at T_{Si} = 200 K, while τ for the low temperature CNT is maximal at the same T_{Si}. The permanent deformation in the CNT was quantified as b which is plotted as a function of T_{Si} in Figure 4b. b for the high temperature CNT generally increases with raising T_{Si} while $b$is not a monotonic function of T_{Si} for the low temperature CNT. On the whole, b is greater for the high temperature CNT, but this difference is small.

Moving on to the dynamics of vibrational temperature, τ_{vib}

was plotted as a function of T_{Si} in Figure 4c. τ_{vib} ranged from 6.6 to 9.3 ps for T_{CNT} = 100 K and from 8.0 to 9.6 ps for T_{CNT} = 300 K. On the whole, τ_{vib} is greater for the high temperature CNT as found for τ above, implying that the vibrational relaxation is faster for the low temperature CNT. No clear trend is found for its dependence on T_{Si}, although it seems decreasing with the rise in T_{Si} for the low temperature CNT. Figure 4d plots b_{vib}, as a function of T_{Si}. b_{vib} increases with the rise in T_{Si}, regardless of T_{CNT}. b_{vib} increases from 183 to 450 K in the case of T_{CNT} = 100 K and from 219 to 389 K for T_{CNT} = 300 K. Interestingly, the low temperature CNT (T_{CNT} = 100 K) has b_{vib}s higher than those of the high temperature CNT. Presumably, heat is transferred from the surface to the low temperature CNT, giving an increased vibrational temperature. On the other hand, a high temperature CNT dissipates its energy to the surface and therefore has a lower value of b_{vib}.

Conclusion

By using MD simulation, we studied the temperature dependent deposition of CNTs on a silicon surface *via* collision. By focusing on the collision geometry where the CNT impacts onto the surface along its long axis, we investigated the effects of the CNT temperature and the surface temperature. The CNT was vertically aligned on the surface and penetrated up to a depth of 1.2 nm at a projectile speed v_p = 5 km/s. Due to its high mechanical resilience, the CNT shows only a small deformation localized at its bottom contacting the surface. The structural and energy relaxation of the low temperature CNT was more efficient (faster) than that of the high temperature CNT. The vibrational temperature of CNT increased with the rise in the surface temperature, regardless of its temperature. A low temperature CNT ended up with a higher vibrational temperature after collision than a high temperature CNT. This is probably due to the possible heat transfer from the surface to the CNT *via* collision.

By averaging over the entire atoms of CNT in calculating the RMSD and vibrational temperature, we left out the dynamics of intramolecular vibrational energy redistribution (IVR). A study of IVR *via* a normal or local mode analysis will elucidate the pathways of the energy (heat) transfer from the bottom to top of CNT after impact. We leave this IVR study as an interesting future work.

Acknowledgments. This work was supported for two years by a Pusan National University Research Grant.

References

1. Ye, H.; Lam, H.; Titchenal, N.; Gogotsi, Y.; Ko, F. *Appl. Phys. Lett.* **2004**, *85*, 1775.
2. Siegel, R. W.; Chang, S. K.; Ash, B. J.; Stone, J.; Ajayan, P. M.; Doremus, R. W.; Schadler, L. S. *Scripta Materialia* **2001**, *44*, 2061.
3. Thostenson, E. T.; Ren, Z.; Chou, T.-W. *Composites Science and Technology* **2001**, *61*, 1899.
4. Cha, S. I.; Kim, K. T.; Lee, K. H.; Mo, C. B.; Hong, S. H. *Scripta Materialia* **2005**, *53*, 793.
5. Qi, D.; Hinkley, J.; He, G. *Modelling Simul. Mater. Sci. Eng.* **2005**, *13*, 493.
6. Frankland, S. J. V.; Harik, V. M.; Odegard, G. M.; Brenner, D. W.; Gates, T. S. *Composites Science and Technology* **2003**, *63*, 1655.
7. Mylvaganam, K.; Zhang, L. C. *Appl. Phys. Lett.* **2006**, *89*, 123127.
8. Laha, T.; Agarwal, A. *Materials Science and Engineering A* **2008**, *480*, 323.
9. Laha, T.; Agarwal, A.; Mckechnie, T.; Seal, S. *Materials Science and Engineering A* **2004**, *381*, 249.
10. Li, C.-J.; Li, W.-Y.; Wang, Y.-Y. *Surface and Coatings Technology* **2005**, *198*, 469.
11. Balani, K.; Laha, T.; Agarwal, A.; Karthikeyan, J.; Munroe, N. *Surface and Coatings Technology* **2005**, *195*, 272.
12. Bakshi, S. R.; Singh, V.; McCartney, D. G.; Seal, S.; Agarwal, A. *Scripta Materialia* **2008**, *59*, 499.
13. Bakshi, S. R.; Singh, V.; Balani, K.; McCartney, D. G.; Seal, S.; Agarwal, A. *Surface and Coatings Technology* **2008**, *202*, 5162.
14. Lopez, M. J.; Cabria, I.; March, N. H.; Alonso, J. A. *Carbon* **2005**, *43*, 1371.
15. Liew, K. M.; Wong, C. H.; He, X. Q.; Tan, M. J. *Phys. Rev. B* **2005**, *71*, 075424.
16. Che, J.; Cagin, T.; Goddard, W. A. *Nanotechnology* **2000**, *11*, 65.
17. Bi, K.; Chen, Y.; Yang, J.; Wang, Y.; Chen, M. *Physics Letters A* **2006**, *350*, 150.
18. Cheng, M.; Lu, Y. *IEEE Transactions on Magnetics* **2006**, *42*, 891.
19. Yin, H.; Luo, C. *Modelling Simulation Mater. Sci. Eng.* **2005**, *13*, 1403.
20. Saha, L. C.; Mian, S. A.; Kim, H.; Jang, J. *J. Phys. Chem. C* **2009**, *113*, 16668.
21. Allen, M. P.; Tildesley, D. J. *Computer Simulation of Liquids*; Clarendon Press: Oxford, U.K, 1987.
22. Tersoff, J. *Phys. Rev. B* **1989**, *39*, 5566.
23. Zhao, J.-X.; Ding, Y.-H. *J. Chem. Theory Comput.* **2009**, *5*, 1099.
24. Smith, W.; Yong, C. W.; Rodger, P. M. *Mol. Simul.* **2002**, *28*, 385.
25. Kabsch, W. *Acta Crystallogr. Sect. A* **1978**, *34*, 827.
26. Humphrey, W.; Dalke, A.; Schulten, K. *J. Mol. Graphics* **1996**, *14*, 33.